Journal of Molecular Liquids 312 (2020) 113331

Contents lists available at ScienceDirect

Journal of Molecular Liquids

journal homepage: www.elsevier.com/locate/molliq

Salting out in ACN/water systems: Hofmeister effects and partition of quercetin

Safar A. Jafari [a], Mohammad H. Entezari [a,b,*]

[a] Sonochemical Research Center, Department of Chemistry, Faculty of Science, Ferdowsi University of Mashhad, Mashhad, Iran
[b] Environmental Chemistry Research Center, Department of Chemistry, Faculty of Science, Ferdowsi University of Mashhad, Mashhad, Iran

ARTICLE INFO

Article history:
Received 1 May 2019
Received in revised form 23 March 2020
Accepted 8 May 2020
Available online 20 May 2020

Keywords:
Salting-out extraction
Quercetin
Acetonitrile
Free energy
Hofmeister series

ABSTRACT

In order to obtain a better understanding of the interaction between acetonitrile and secondary plant metabolites, partition behavior of quercetin as a biomolecule model was investigated in systems composed of acetonitrile, salt [NaCl/KCl/NaBr/KBr], and water at different temperatures. The salting-out ability of the constituent anions and cations of these salts followed the well-known Hofmeister series and the effect of anion was more pronounced than the effect of cation. The Setschenow-type equation is applied to study the slating-out effects on the selected systems. The effect of temperature on the cloud-points as a function of acetonitrile mole fraction was studied in the temperature range of 293.15–328.15 K at 5 K intervals in aqueous solution of acetonitrile. The results showed that the concentration of acetonitrile in equilibrium with a certain concentration of salts significantly increased by the increasing of temperature. The free energy, enthalpy and entropy changes of clouding point (CP) was estimated by using a simple method and the driving force of formation of two phases may be the decrease of enthalpy. Investigation of the distribution behavior of quercetin showed that with increasing the salting-out ability of salt, IC_{50} values (the concentration necessary for 50% reduction of DPPH) of bottom phases, partition coefficient and recovery of quercetin significantly increased. The effect of temperature on the recovery of quercetin showed that the recovery decreased with the increasing of temperature in total systems under investigation and the decrease more significantly for bromide salts. The change in Gibbs energy (ΔG_t), enthalpy (ΔH_t) and entropy (ΔS_t) of quercetin transfer process was calculated from the partition data. The results confirmed that under the same conditions with increasing the salting-out ability of salt, the calculated ΔG_t values were more negative.

1. Introduction

Secondary metabolites such as quercetin (3, 3′, 4′, 5, 7-pentahydroxy flavone) as a biomolecule are organic compounds produced by plants. Due to the antioxidant activity, secondary metabolites are essential components in a variety of nutraceutical, pharmaceutical, medicinal and cosmetic applications [1]. High Performance Liquid Chromatography (HPLC) is used in a variety of industrial and scientific applications, such as pharmaceutical, chemicals and environmental. Quantitative and qualitative analysis of secondary plant metabolites often is carried out in the pharmaceutical industry by HPLC. Acetonitrile (ACN) is solvent that is commonly used in reversed-phase HPLC for secondary metabolites analysis [2]. In order to obtain a better understanding of the interaction between acetonitrile and secondary metabolites, partition behavior of quercetin as a model biomolecule was investigated in systems composed of acetonitrile, salt, and water at different temperatures. Quercetin with specific structure acts as a powerful antioxidant. It is a bioactive flavonoid compound and is found abundantly in vegetables and fruits. There is growing evidence suggesting that quercetin has therapeutic potential for the prevention and treatment of different diseases [3]. Quercetin bioavailability depends on the type of glycosides present in different food sources. Studies have demonstrated that the adsorption of quercetin glycosides almost twice as much as its corresponding aglycon [4].

As it mentioned, ACN is a key solvent in the chemical industries, particularly the pharmaceutical industry [5], where the global demand accounts for over 70% of the total market. ACN Market size was valued at United States Dollar (USD) 209.1 Million in 2016 and projected to reach USD 277.1 Million by 2022, at a compound annual growth rate of 4.8% during the forecast period. The high popularity of ACN is due to its excellent solvation ability with respect to a wide range of polar and non-polar solutes, and favorable properties such as low freezing/boiling points, low viscosity and relatively low toxicity. Therefore, shortage of ACN in

* Corresponding author at: Sonochemical Research Center, Environmental Chemistry Research Center, Department of Chemistry, Faculty of Science, Ferdowsi University of Mashhad, Mashhad, Iran.
E-mail address: entezari@um.ac.ir (M.H. Entezari).

https://doi.org/10.1016/j.molliq.2020.113331
0167-7322/

the future combined with environmental challenges requires recovery of ACN from aqueous waste. "Salting out" is an innovative technique for recovery of ACN from aqueous waste.

More than 100 years ago, Hofmeister measured the concentrations of various salts needed to precipitate proteins from whole egg white [6,7]. Nowadays this effect is known as the Hofmeister effect. It is very general and can be used to alter the solubility of a wide range of organic compounds miscible with water in mixed solvent systems.

The mixed solvent system in the presence of an added electrolyte is an attractive technology to study. When the concentration of the added salt exceeds from a critical value, the one-phase mixed solvent system becomes an immiscible biphasic system. In this biphasic system, the concentration of the constituents of the phases is different. If one of the phases is water, the system is known as an aqueous two-phase system (ATPS) [8].

Liquid-liquid equilibria (LLE) in $ATPS_S$ are the result of intermolecular forces, predominantly hydrogen bonding [9]. Addition of a salt to such a system introduces ionic forces that alter the structure of the liquids in equilibrium. The water molecules that surround the ions become unavailable for the organic solvent and it becomes "salted out" from the aqueous phase. On the other hand, the salting out effect is utilized for facilitating the separation of organic compounds from aqueous solutions.

ATPS composed of an organic solvent and a salt solution have been used to isolate pharmaceutical ingredients [10–13]. Advantages of using this system are lower viscosity, lower cost of chemicals and shorter phase separation time. Therefore, in this work, the use of ACN-salt-based ATPS was investigated as an alternative platform for recovery of quercetin.

Phase equilibria in an aqueous biphasic system containing ACN have been investigated by several researchers. For example, salting-out effect of sodium, potassium, carbonate, sulfite, tartrate and thiosulfate ions was studied in aqueous mixtures of ACN [14], and novel $ATPS_S$ composed of ACN and polyols [15]. As far as we know, there is no report that systematically investigate LLE along with its application for ACN and aqueous solution of sodium chloride, potassium chloride, sodium bromide and potassium bromide salts. In this work, first, LLE for ACN and aqueous solution of different salts was investigated. Then, quercetin was used as a model biomolecule for partitioning in ATPS. In order to propose a potential strategy for the extraction and purification of quercetin biomolecule, investigation was carried out on the partitioning behavior of quercetin. The main effective parameters such as kind of salt and temperature on the ATPS were studied to obtain a higher partition coefficient and higher extraction efficiency of quercetin. Finally, in order to confirm the results, salt effect was investigated on the antioxidant capacity of both phases in the systems (quercetin solution ($1.0\ g\cdot kg^{-1}$ ACN) + salt + water).

2. Material and methods

2.1. Materials

ACN (GR, 99.5%) was obtained from Sumchun, NaCl (GR, 99.5%), NaBr (GR, 99.5%), and KBr (GR, min 99.5%) were obtained from Merck. KCl (GR, 99%) from Fluka, aluminum chloride hexahydrated (98%), sodium nitrite (min 99.99%), quercetin (min 95%), and 2, 2-diphenyl-1-picrylhydrazyl (DPPH; 97%) were purchased from Sigma-Aldrich. These reagents were used without further purification and doubly distilled deionized water was used in all experiments.

2.2. Phase diagrams and tie lines

The experimental apparatus employed in this work is essentially similar to the one used before [16]. A double wall glass vessel is used for carrying out the binodal curve measurements on a magnetic stirrer plate. It was provided with an external jacket in which water at constant temperature (±0.1 °C) is circulated from a refrigerated bath circulator (DAIHAN model WCR—P22, Korea). The binodal curves were determined by the cloud point method. An aqueous salt solution of know concentration was titrated with ACN, until the solution turned turbid, which indicated the formation of two liquid phases. The solution was back titrated by adding water until the turbidity was vanished. The composition before the addition of the last drop before clearing was a point on the binodal curve. The composition of the mixture was followed by mass using an analytical balance (Sartorius model TE214S, Switzerland) with a precision of $\pm 1 \times 10^{-4}$ g. This procedure continued for other binodal points too.

The tie-lines (TLs) were obtained through a gravimetric method originally described by Merchuk and co-workers [17]. The feed samples (about 10 g) were prepared by mixing appropriate amounts of ACN, salt, and water in the conical vessel that are in the biphasic region. These samples were stirred ($1500\ cycles\cdot min^{-1}$) using a stirrer (RCTB, IKA) for 10 min. Feed samples were immersed in a thermostated water bath at constant temperature 25 °C. Based on the thermodynamics, under equilibrium conditions, any macroscopic property of the systems is stable, and therefore to ensure the occurrence of the thermodynamic equilibrium. The refractive index and mass of some samples of the both phases (i.e. salt-rich and ACN-rich) of several feed samples were measured using a refractometer (CARL ZEISS, Germany) with an uncertainty of the ±0.0002 and analytical balance. The periodic measurements showed that the necessary rest time to ensure the thermodynamic equilibrium is about 20 min. However, the feed samples were immersed in the water bath for about 2 to 3 h to enrich the equilibrium condition. After equilibrium was achieved, samples were carefully withdrawn using long needle syringes. For withdrawing bottom phase, a tiny bubble of air was retained at the needle tip and expelled in the bottom phase to prevent contamination from upper phase material. After the separation of two phases, the mass of both phases was determined by analytical balance. The mass of both phases for determination of phase compositions was given in supplementary file (Table S1). Each individual TL was determined by the application of the lever-arm rule, which describes the relationship between the weight of the top phase and the overall system weight and composition. For that purpose, the binodal curves were fitted to the obtained experimental data according to Eq. (1).

$$W_1 = \mathrm{Exp}\left(U_0 + U_1(W_2)^{0.5} + U_2(W_2)^3\right) \tag{1}$$

where, W_1 and W_2 are the weight fraction percentages of ACN and salt, respectively; and U_0, U_1, U_2 are the fit coefficients of Eq. (1). Then, the determination of the tie lines was accomplished by solving the following equations (Eqs. (2)–(5)) simultaneously, for the four unknown values W_{1bp}, W_{1tp},W_{2bp} and W_{2tp}.

$$W_{1tp} = \mathrm{Exp}\left(U_0 + U_1(W_{2tp})^{0.5} + U_2(W_{2tp})^3\right) \tag{2}$$

$$W_{1bp} = \mathrm{Exp}\left(U_0 + U_1(W_{2bp})^{0.5} + U_2(W_{2bp})^3\right) \tag{3}$$

$$W_{1tp} = \frac{W_{1tc}}{\alpha} - \frac{(1-\alpha)W_{1bp}}{\alpha} \tag{4}$$

$$W_{2tp} = \frac{W_{2tc}}{\alpha} - \frac{(1-\alpha)W_{2bp}}{\alpha} \tag{5}$$

where the subscripts tp, bp and tc denote, the top phase, bottom phase and total composition, respectively. The value of α is the ratio between the mass of the top phase and the total weight of the system. The simultaneous solution of the Eqs. (2)–(5) led to the ACN and salt weight fraction percentages in the top and bottom phases. Thus, TLs can simply

Please cite this article as: S.A. Jafari and M.H. Entezari, Salting out in ACN/water systems: Hofmeister effects and partition of quercetin, Journal of Molecular Liquids, https://doi.org/10.1016/j.molliq.2020.113331

represent and the respective tie-line lengths (TLLs) can be determined through the application of Eq. (6).

$$TLL = \sqrt{(X_{1tp} - X_{1bp})^2 + (X_{2tp} - X_{2bp})^2} \quad (6)$$

where X_1 and X_2 are the mole fraction percentages of ACN and salt, respectively. The simple gravimetric method used in this work is the basis of determination of tie lines and binodal that are mass measurements. Therefore, the accuracy and repeatability of this method is very high.

For the effects of temperature on the cloud-point, an aqueous salt solution of know concentration was titrated with ACN, until the solution turned turbid. Then, temperature increased at 5 K intervals until the turbidity vanished, and the addition of ACN was repeated until the solution turned turbid again. In this work, the relative mole fraction of two components remained constant and the mole fraction of the third component (ACN) was changed.

2.3. Quercetin concentration

After systematic studies on the liquid−liquid equilibrium behavior of aqueous solutions shown in Fig. 9A, the partition behavior of quercetin was followed in these systems. Biphasic systems (quercetin solution ($1.0\ g \cdot kg^{-1}$ ACN) + salt + water) were prepared in the vessel with the same previous total composition. The samples were stirred ($1500\ cycles \cdot min^{-1}$) for 10 min. and then immersed in a water bath (thermostat) at constant temperature for about 20 min to reach an equilibrium. When an equilibrium was achieved, samples were carefully withdrawn using long needle syringes. After the separation of the two phases, the mass of both phases was determined by analytical balance within $\pm 10^{-4}$ g. The method described by Zhishen et al. with minor modifications applied in this work to determine quercetin concentration in both phases [18]. The amount of 50 mg of quercetin was dissolved in ACN and then diluted to 100–1000 ppm. To 0.50 g of the suitably diluted sample, 0.30 g of a 5% $NaNO_2$ solution, 0.30 g of a freshly prepared 10% $AlCl_3$ solution, and 1 g of 1 M NaOH solution were added. The final mass was adjusted to 4 g with ethanol (50%). After incubation at room temperature for 30 min and complexation with $AlCl_3$, the absorbance of the reaction mixture was measured at 465 nm using a UV-VIS spectrophotometer (UV-2800, Unico, USA). The same sample without $AlCl_3$ was used as a blank solution. Similarly, the certain mass of phases was reacted with aluminum chloride for determination of quercetin concentration as was described above. The quercetin concentration was calculated using the following linear equation based on the calibration curve:

$$A = 0.007C + 0.016 \qquad R^2 = 0.998 \quad (7)$$

where A is the absorbance and C is the quercetin concentration in $\mu g \cdot g^{-1}$. In the determination of quercetin concentration by above procedure, percentage of average quercetin recovery in both phases under investigation was 96.84% of initial quercetin content. Therefore, the accuracy and repeatability of this method is high.

2.4. Antioxidant capacity of phases

The antioxidant capacity of phases was assessed using DPPH radical according to the literature with moderate modification [19]. A certain mass of both phases solution was diluted with DPPH methanol solution (0.10 mM) until ultimate mass of 3 g. Acetonitrile solutions 80% for top phase and 20% for bottom phase were used instead of phase solutions in the blank system. The most concentrated phase solution (0.30 g) was added into 2.70 g DPPH methanol solution as control sample. The mixture was shaken vigorously and left to stand for 60 min at ambient temperature in darkness. Absorbance was determined at 517 nm. The results were expressed as percentage inhibition of the DPPH radical and calculated using the following equation.

$$\text{Antioxidant capacity} = \left(1 - \frac{A_s - A_C}{A_b}\right) \times 100 \quad (8)$$

where A_c, A_s and A_b represent the absorbance of control, sample and blank, respectively. The antioxidant capacity of phases was expressed as IC_{50} that calculated from the plots of percent inhibition versus phase solution concentration.

3. Results and discussion

3.1. Phase diagrams

The experimental binodal curves data for (ACN) + Salt (NaCl, KCl, NaBr, KBr) + Water ternary systems at 25 °C are reported in Table S2 and tie-line compositions with TLL are reported in Table 1. Furthermore, the phase diagrams for these systems are shown in Figs. 1–4. The comparison of binodal curves is depicted in Fig. 5 at 25 °C.

3.2. Effect of different salts on the phase diagram

From Fig. 5 it is obvious that, the two-phase formation ability of the systems composed of ACN follows the ordering NaCl > KCl > NaBr > KBr. This observation is discussed based on the changes in the intermolecular interactions between the components of the system when an electrolyte and an organic solvent is mixed in an aqueous solution. The “hydration theories” can describe a simple representation of the salting-out phenomenon. Based on these theories [20], when the electrolyte is solved in a solvent the stronger ion-solvent interactions overcome the ion-ion interactions. Then, the distance between the ions increases and consequently, each of the constitutive ions of the electrolyte is surrounded by a layer of solvent. The stronger solvation interactions immobilize the solvent molecules and suppress their role as solvent. In an organic solvent and aqueous electrolyte system, the organic solvent molecules and

Table 1
Tie line data and tie line length (TLL) for the ACN (1) + Salt (2) + Water (3) systems as mole fraction percent at 25 °C.

Total composition		Top phase		Bottom phase		TLL
$100x_1$	$100x_2$	$100x_1$	$100x_2$	$100x_1$	$100x_2$	
ACN (1) + NaCl (2) + Water (3)						
26.97	1.50	59.88	0.19	15.49	1.95	44.43
29.99	1.75	65.49	0.15	12.86	2.52	52.68
31.86	1.93	67.96	0.13	11.65	2.94	56.38
36.03	2.26	70.29	0.12	10.27	3.86	60.14
38.93	2.50	72.69	0.10	10.07	4.54	62.77
ACN (1) + KCl (2) + Water (3)						
29.95	1.75	64.12	0.18	14.62	2.46	49.55
32.46	1.97	67.05	0.16	12.80	3.00	54.32
35.82	2.23	71.82	0.13	11.44	3.66	60.48
38.98	2.54	72.78	0.12	11.07	4.58	61.86
40.86	2.68	74.15	0.11	10.44	5.03	63.90
ACN (1) + NaBr (2) + Water (3)						
30.03	1.75	52.06	0.82	24.59	1.98	27.49
33.04	2.01	61.27	0.67	19.64	2.64	41.68
35.98	2.25	66.70	0.60	17.12	3.26	49.65
39.03	2.50	70.68	0.56	15.65	3.94	55.13
41.99	2.75	72.54	0.54	15.07	4.69	57.61
ACN (1) + KBr (2) + Water (3)						
33.85	2.08	54.54	0.87	23.90	2.66	30.69
36.01	2.25	60.11	0.76	21.18	3.17	39.00
39.00	2.50	65.44	0.67	18.54	3.91	47.01
41.97	2.75	69.05	0.62	16.82	4.73	52.39
44.94	3.00	74.53	0.55	15.99	5.39	58.74

Please cite this article as: S.A. Jafari and M.H. Entezari, Salting out in ACN/water systems: Hofmeister effects and partition of quercetin, Journal of Molecular Liquids, https://doi.org/10.1016/j.molliq.2020.113331

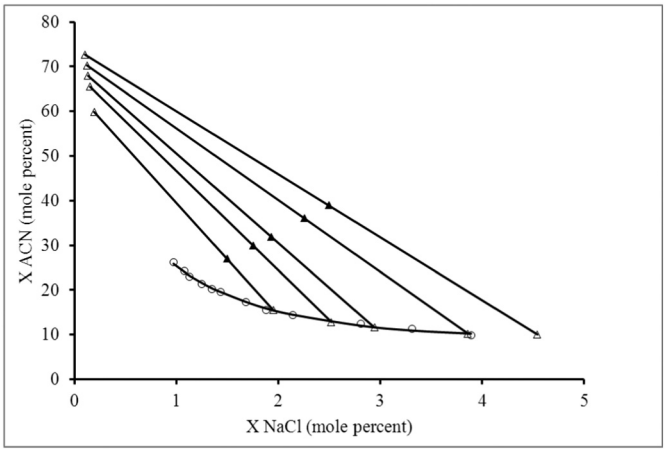

Fig. 1. Binodal curve and tie lines for ACN (1) + NaCl(2) + Water (3) at 25 °C: ○, experimental data of the binodal curve; —, calculated from Eq. (1); △, tie line data; ▲, initial total composition.

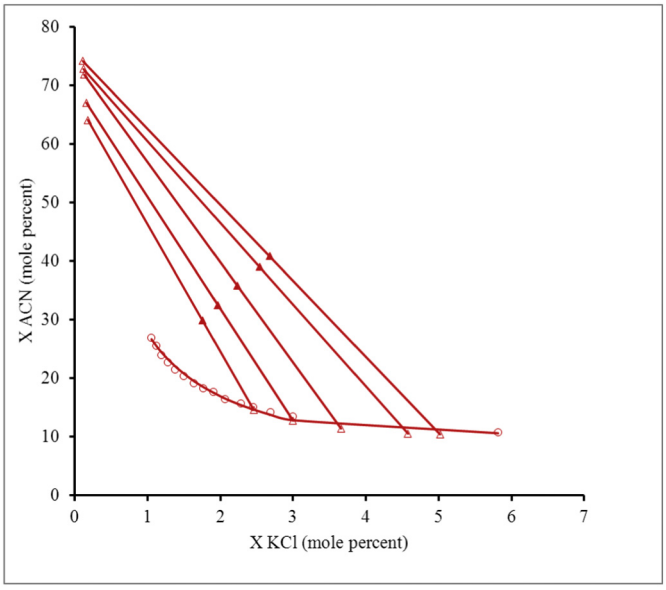

Fig. 2. Binodal curve and tie lines for ACN (1) + KCl(2) + Water (3) at 25 °C: ○, experimental data of the binodal curve; —, calculated from Eq. (1); △, tie line data; ▲, initial total composition.

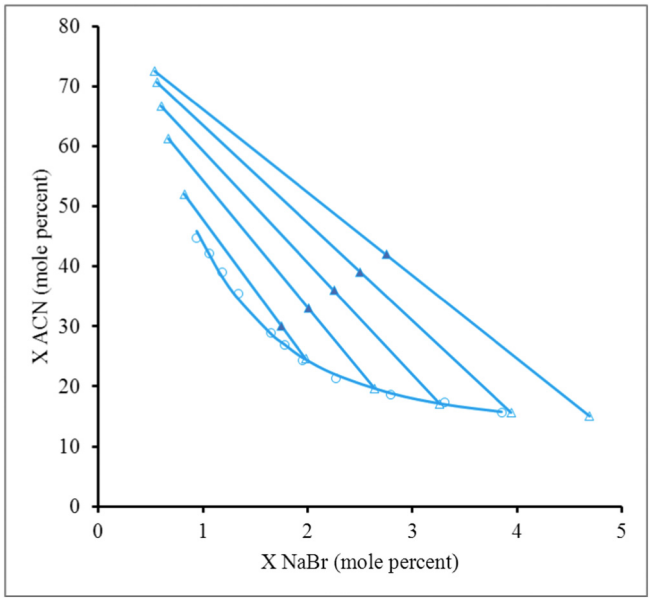

Fig. 3. Binodal curve and tie lines for ACN (1) + NaBr (2) + Water (3) at 25 °C: ○, experimental data of the binodal curve; —, calculated from Eq. (1); △, tie line data; ▲, initial total composition.

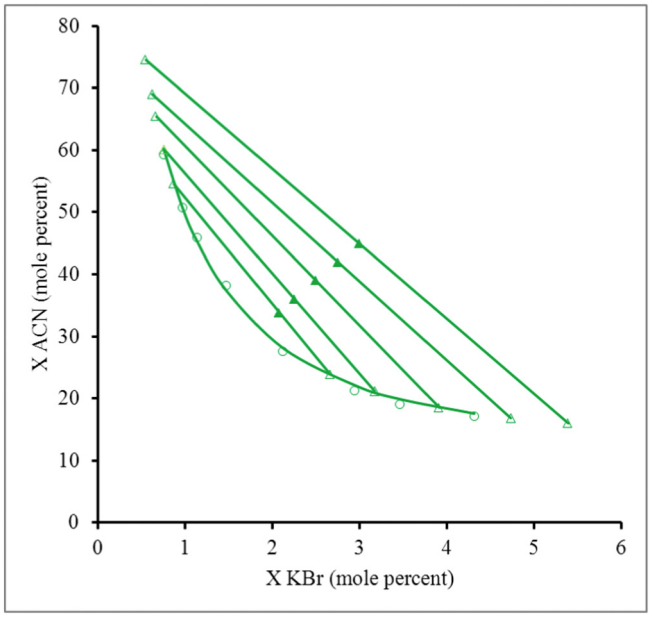

Fig. 4. Binodal curve and tie lines for ACN (1) + KBr (2) + Water (3) at 25 °C: ○, experimental data of the binodal curve; —, calculated from Eq. (1); △, tie line data; ▲, initial total composition.

dissolved ions compete with each other to detain more solvent (i.e. water) molecules around their respective hydration shells. In this challenge, the ionic species have more interactions with water molecules. They can achieve more water molecules and proportionally the other component enforced to decrease the interactions with water molecules and therefore its self-intermolecular interactions increased. Subsequently, the organic solvent is "salted out" and when the amount of electrolyte increased from the specific threshold concentration, the organic solvent molecules excluded from the remained solution as a separated phase. Therefore, from Fig. 5 can be concluded that, the salting-out ability of the constituent anions and cations of these salts is as follows: $Na^+ > K^+$ and $Cl^- > Br^-$. Indeed, the cation and anion influence in the salting-out of the ACN follows the well-known Hofmeister series [7,21,22]. Fig. 5 also shows that the difference between the effects of Cl^- and Br^- anions on the salting-out of the ACN in the presence of a fixed cation is more pronounced than the effects of Na^+ and K^+ cations in the presence of a fixed anion. This difference has been attributed to the higher polarizability, relatively larger size and different hydration characteristics of anions compared to those of cations [23].

The salting out ability of different salts is attributed to the Gibbs free energy of hydration, ΔG_{hyd}, of the constituent ions. ΔG_{hyd} is the change in the free energy from an isolated naked ion in the gas phase to the aqueous hydrated ion in solution. Therefore, the ions with higher kosmotropicity have a more negative ΔG_{hyd}, due to the resulting more structured water 'lattice' around the ion [24]. Marcus [25] reported the experimental values of −365, −295,-340 and −315 $kJ \cdot mol^{-1}$ for ΔG_{hyd} of Na^+, K^+, Cl^- and Br^-, respectively. Comparison of ΔG_{hyd} values and the salting-out abilities represented above, shows that the more negative value of ΔG_{hyd} of the cation or anion results in the more salting-out ability of the ion.

Please cite this article as: S.A. Jafari and M.H. Entezari, Salting out in ACN/water systems: Hofmeister effects and partition of quercetin, Journal of Molecular Liquids, https://doi.org/10.1016/j.molliq.2020.113331

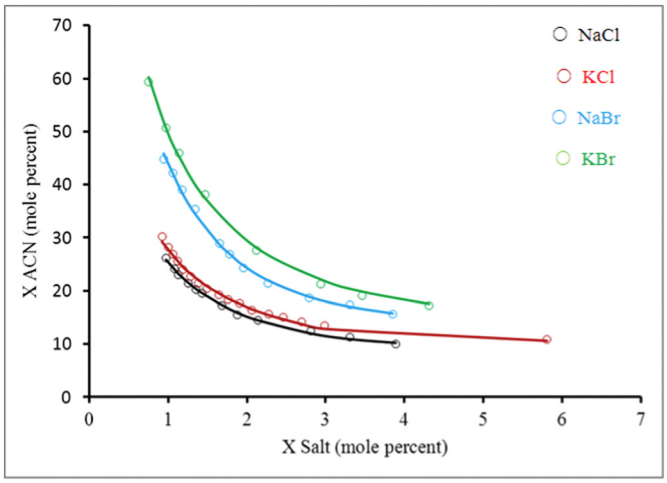

Fig. 5. Comparison of binodal curves for the ACN (1) + Salt (2) + Water (3) systems at 25 °C: –, calculated from Eq. (1).

3.3. Cloud-point (CP) data and thermodynamic parameters

The temperature behavior of the investigated aqueous two-phase systems can further illustrated if we consider the diagram of cloud-point temperature as a function of ACN mole fraction. The CP temperature as a function of ACN mole fractions measured in the temperature range of 293.15–328.15 K at 5 K intervals on the investigated systems. The experimental CP data were reported in Table S3 and plotted in Fig. 6. It shows that the concentration of acetonitrile that is in equilibrium with a certain concentration of salts significantly increases by increasing temperature. In other words, the phase-separation ability of all studied ATPS$_s$ in the temperature range of 293.15–328.15 K decreases with increasing the temperature. In another point of view, in these systems by the increasing temperature, the electrostatic interactions between ionic species and water molecules decrease and thus, more ACN mole fraction is required for phase separation. As shown in Fig. 6, the bromide salts are more sensitive to higher temperatures so that for potassium bromide salt, with the lowest salting-out abilities at temperatures of 313.15 K or above, phase separation does not occur.

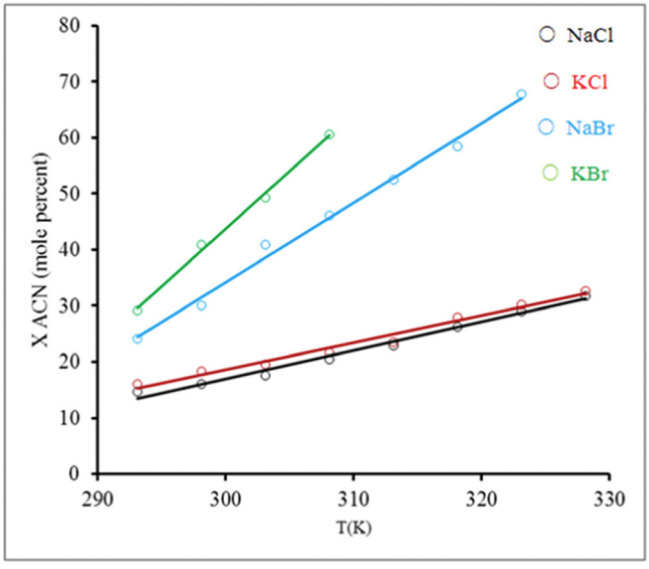

Fig. 6. Effect of temperature on cloud point, CP, as ACN mole fraction, in the presence of aqueous solution of salts. –, calculated from Eq. (12).

Recently, Dan et al. [26], considering CP as the point of phase separation (or the solubility limit) estimated the free energy, ΔGc, enthalpy, ΔHc, and entropy, ΔSc, of phase-separation to obtain some information about the driving force of the aqueous two phase formation process. Dan et al., the free energy of phase separation or clouding (ΔG_c) calculated from the following equation:

$$\Delta G_c = RT\ln X_1 \tag{9}$$

where X_1 is the mole fraction of the ACN at CP. The ΔG_c values are calculated using the experimental CP values of ACN for the same salt to water mole fraction ratios and reported in Table 2. The ΔG_c values at different CP (or T) are processed according to the equation given below to get ΔH_c from the slope of the linear (least squares) plot of $(\frac{\Delta Gc}{T})$ against $(\frac{1}{T})$ for each of the studied ATPS$_s$:

$$\Delta Hc = \frac{d\left(\frac{\Delta G}{T}\right)}{d\left(\frac{1}{T}\right)} \tag{10}$$

The calculated ΔH_c values presented in Table 2 are negative for all studied ATPS$_s$. The negative values of ΔH_c for these systems demonstrate that the phase-separation process is an exothermic process.

Moreover, the following equation was used to calculate the entropy changes of phase-separation:

$$\Delta G_c = \Delta H_c - T\Delta S_c \tag{11}$$

The calculated values of ΔH_c and $T\Delta S_c$ from Eqs. (10) and (11) were reported in Table 2, which are negative. Therefore the driving force of two phase formation process may be the decrease of enthalpy.

In this work, the following simple empirical equation was used to represent the studied cloud point temperatures:

$$X_1 = S_0 + S_1 T_c \tag{12}$$

where T_c, and X_1 represent the cloud point temperature and mole fraction percent of ACN, respectively. The coefficients of Eq. (12) along with the corresponding standard deviations for the investigated systems are given in Table S4. The standard deviations calculated using the following equation, where N is the number of data.

$$\sigma_{(X)} = \sum_{i=1}^{N}\left(\frac{(X_{i,cal} - X_{i,exp})^2}{N}\right)^{0.5} \tag{13}$$

3.4. Modeling of the phase diagrams

3.4.1. Correlation of the binodal curves

The experimental binodal pointes were correlated using Eq. (1), and the obtained parameters along with the corresponding standard deviations were reported in Table 3. Figs. 1–4 compare the experimental points and calculated binodal curves for the studied ATPS$_s$. Base on the standard deviations reported in Table 3 and the results shown in Figs. 1–4, it is concluded that, Eq. (1) successfully correlates the binodal curves of the investigated systems with experimental points. The standard deviations were calculated using the following equation, where N is the number of binodal data.

$$\sigma_{(X)} = \sum_{i=1}^{N}\left(\frac{(X_{i,1,cal} - X_{i,1,exp})^2}{N}\right)^{0.5} \tag{14}$$

3.4.2. Correlation of the tie-lines data

Over a century ago, Setschenow derived an empirical equation to describe salting out ability of different salts [27]. Since then, considerable efforts have made to modify this empirical equation [28,29]. Currently,

Table 2
Cloud-point (*CP*) data along with the calculated ΔG, ΔH and ΔS for the ACN (1) + salt (2) + Water (3) systems as a function of mole fraction of the ACN at different temperatures.

T/K	293.15	298.15	303.15	308.15	313.15	318.15	323.15	328.15
System	ACN (1) + NaCl (2) + Water (3) $\frac{X_2}{X_3} = 0.02383$							
X_{ACN}	0.147	0.160	0.176	0.205	0.228	0.263	0.291	0.317
$\Delta G(kJ\cdot mol^{-1})$	−4.67	−4.55	−4.38	−4.06	−3.84	−3.53	−3.32	−3.13
$\Delta H(kJ\cdot mol^{-1})$	−18.46							
$T\Delta S(kJ\cdot mol^{-1})$	−13.79	−13.91	−14.08	−14.39	−14.61	−14.93	−15.14	−15.33
System	ACN (1) + KCl (2) + Water (3) $\frac{X_2}{X_3} = 0.02411$							
X_{ACN}	0.161	0.182	0.196	0.217	0.235	0.279	0.302	0.326
$\Delta G(kJ\cdot mol^{-1})$	−4.46	−4.22	−4.11	−3.91	−3.77	−3.37	−3.22	−3.06
$\Delta H(kJ\cdot mol^{-1})$	−16.41							
$T\Delta S(kJ\cdot mol^{-1})$	−11.95	−12.19	−12.30	−12.50	−12.65	−13.04	−13.19	−13.36
System	ACN (1) + NaBr (2) + Water (3) $\frac{X_2}{X_3} = 0.02376$							
X_{ACN}	0.241	0.301	0.409	0.461	0.524	0.585	0.678	
$\Delta G(kJ\cdot mol^{-1})$	−3.47	−2.98	−2.25	−1.98	−1.68	−1.42	−1.05	
$\Delta H(kJ\cdot mol^{-1})$	−26.41							
$T\Delta S(kJ\cdot mol^{-1})$	−22.94	−23.43	−24.16	−24.42	−24.73	−24.99	−25.36	
System	ACN (1) + KBr (2) + Water (3) $\frac{X_2}{X_3} = 0.02381$							
X_{ACN}	0.291	0.409	0.493	0.605				
$\Delta G(kJ\cdot mol^{-1})$	−3.01	−2.22	−1.78	−1.29				
$\Delta H(kJ\cdot mol^{-1})$	−35.92							
$T\Delta S(kJ\cdot mol^{-1})$	−32.91	−33.70	−34.14	−34.63				

Table 3
Coefficients of Eq. (1) at 25 °C.

System	U_0	U_1	U_2	σ
ACN (1) + NaCl (2) + Water (3)	4.70836	−0.61437	0.00020	0.39
ACN (1) + KCl (2) + Water (3)	4.7176	−0.52239	0.00007	0.58
ACN (1) + NaBr (2) + Water (3)	5.05542	−0.49097	0.00004	0.58
ACN (1) + KBr (2) + Water (3)	4.98828	−0.39795	0.00001	0.70

Setschenow-type equation that has often used for the correlation of the tie-line data [30–34] has the following form.

$$\ln\left(\frac{X_{1tp}}{X_{1bp}}\right) = \beta_2 + K_3\left(X_{2bp} - X_{2tp}\right) \quad (15)$$

where K_3 is the salting-out coefficient, β_2 is a constant and X_1, X_2 represent the mole fraction of organic solvent and salt in the top and bottom phases, respectively.

In our previous work [35], it was confirmed that the salting out effect of the studied systems cannot be described based on the Setschenow-type Eq. (15). The slating-out coefficient of Eq. (15) cannot be used as a criterion for the salting-out ability of different salts. It seems that Eq. (15) can be suitable for the ATPSs composed of polymer + salt + water. For the $ATPS_s$ composed of [alcohol or ACN] + salt + water, a displacement in organic solvent and salt mole fractions can be performed. Therefore, the Eq. (16) was used for the correlation of experimental tie-line data.

$$\ln\left(\frac{X_{2bp}}{X_{2tp}}\right) = \beta_2 + K_3\left(X_{1tp} - X_{1bp}\right) \quad (16)$$

The values of the parameters for the investigated systems have been shown in Table 4. Based on the obtained standard deviations and presented in Table 4, it is concluded that Eq. (16) can be satisfactory used to correlate the tie-line data of the investigated systems. The standard deviations are calculated using the following equation:

$$\sigma_j = \left[\frac{1}{2N}\sum_{i=1}^{N}\left[\left(X_{i,j,cal}^{top} - X_{i,j,exp}^{top}\right) + \left(X_{i,j,cal}^{bot} - X_{i,j,exp}^{bot}\right)\right]\right]^{0.5} \quad (17)$$

where σ_j standard deviation of component j and N is the number of tie-lines.

Fig. 7 shows the linear relationship between $\ln\left(\frac{X_{2bp}}{X_{2tp}}\right)$ values and $(X_{1tp} - X_{1bp})$ in the ternary systems (ACN + Salt [NaCl, KCl, NaBr, and KBr] + Water) at 25 °C. It is observed that the slope of lines for chloride salts is more than bromide and the slope of lines increases with increasing salting-out ability of salt. Therefore, by using Eq. (16) in $ATPS_s$ with almost the same total composition based on mole fraction, salting out ability of different salts can be evaluated quantitatively based on slating-out coefficient (k_3).

Table 4
Coefficients of Eq. (16) at 25 °C.

System	β_2	K_3	$100\sigma_1$	$100\sigma_2$
ACN (1) + NaCl (2) + Water (3)	−1.24	7.88	0.88	0.16
ACN (1) + KCl (2) + Water (3)	−1.51	8.24	0.72	0.17
ACN (1) + NaBr (2) + Water (3)	−0.29	4.12	1.39	0.15
ACN (1) + KBr (2) + Water (3)	−0.21	4.25	0.44	0.05

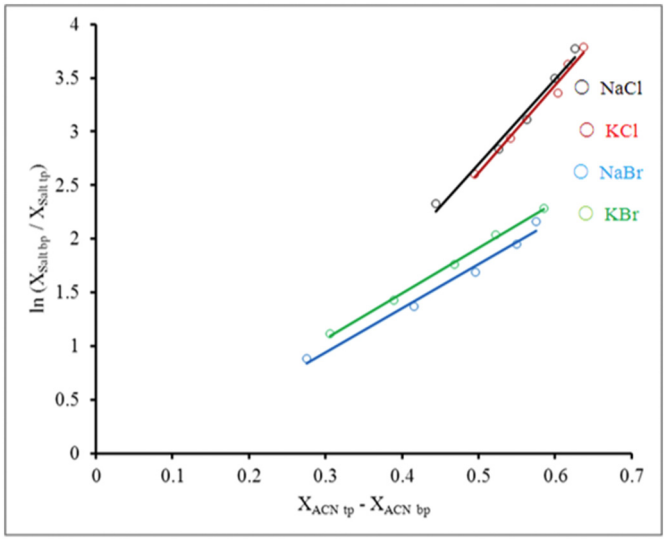

Fig. 7. Setschenow-type plots for the tie-lines data of the [ACN (1) + Salt (2) + Water (3)] system at 25 °C: –, calculated from Eq. (16).

3.5. Salt effects

3.5.1. On absorbance of quercetin

Fig. 8A shows the quercetin structure. The most important structural elements of quercetin are C-3, C-5 and C-7 hydroxyl groups of C and A rings, respectively as scavengers of free radicals. An o-dihydroxy group in the B ring as a radical target and a double bond between positions 2 and 3 of the C-ring conjugated with keto group in position 4 due to its capacity to delocalize the uncoupled electron of a quercetin radical [36]. The absorption spectra of quercetin consist of two distinctive bands in a broad range of 240–400 nm. Band I, covering the range of 240–280 nm (with λ_{max} around 255 nm) attributed to the A–C benzoyl system. Band II, covering the range 300–380 nm is attributed to the B-ring (with λ_{max} around 370 nm) and a weak band with an absorption maximum around 300 nm was also detected which is attributed to the C-ring only [37]. Fig. 8B shows the absorption spectrum of solutions of 100 fold dilution top phases by ACN 80% and 20 fold dilution of bottom phases by ACN 20%. As can be seen, in contrast to the top phase, there is a significant difference in the absorption values of the bottom phase in λ_{max} 255 and 370 nm. On the other hand, with increasing salting-out ability of salt, quercetin migrates along with the acetonitrile into the top phase and concentration of quercetin in bottom phase significantly decreases.

3.5.2. On antioxidant capacity of phases

In Fig. 8C and D, the antioxidant capacity of phases versus mg of phase in g of 0.10 mM DPPH solution are plotted for the top and bottom phases, respectively. In contrast to the top phases, there is

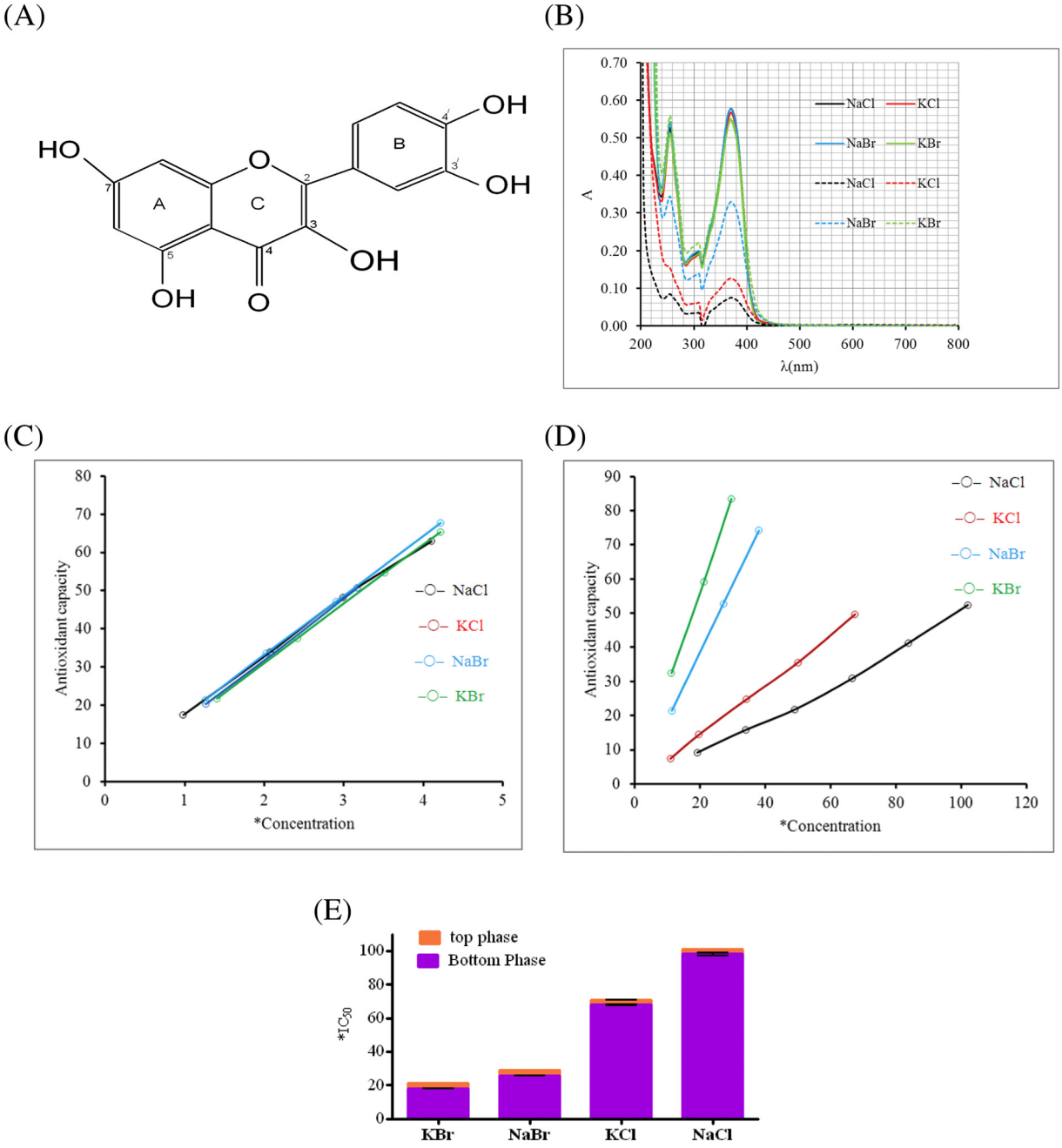

Fig. 8. (A) Quercetin structure. (B) UV–Vis spectra of 100 fold diluted top phases by ACN 80% (solid lines) and 20 fold diluted bottom phases by ACN 20% (dashed lines) for the quercetin solution (1.0 g·kg^{-1} ACN) + Salt + Water systems at 25 °C. (C) and (D) Antioxidant capacity of top and bottom phases for the quercetin solution (1.0 g·kg^{-1} ACN) + Salt + Water systems in 0.10 mM DPPH solution at 25 °C. (E) Comparison of IC_{50} values of top and bottom phases for the same systems at 25 °C. *Phase mg/g 0.10 mM DPPH solution.

a significant difference in the antioxidant capacity of bottom phases, as with increasing salting-out ability of salt, concentration of quercetin and antioxidant capacity in bottom phases decreases. As well as, Fig. 8E represents that in contrast to the top phases, there is a significant difference in the IC_{50} values of bottom phases, as with increasing salting-out ability of salt, IC_{50} values of bottom phase increase.

3.5.3. On tie-line and recovery of quercetin

Recovery percent of quercetin (R) in top phase calculated using the following equation:

$$R = \frac{C_{Q\ tp}}{C_{Q\ initial}} \times 100 \quad (18)$$

where $C_{Q\ tp}$ and $C_{Q\ initial}$ are mg of quercetin in top phase and total mg of quercetin in primary solution, respectively.

Fig. 9A compares the tie lines of the $ATPS_s$ studied in this work. The total composition is almost identical for all four systems, but tie-line length for chloride salts is more than bromide. In other words, with increasing the salting-out ability of salt, ACN mole fraction in top phase and salt mole fraction in bottom phase increases. Fig. 9B represents that with increasing the salting-out ability of salt, tie-line length and recovery of quercetin increases. The obtained results indicate that quercetin preferentially is enriched into the ACN-rich top phase for all the systems studied. Therefore, an increase in salting-out ability of salt and tie line length decreases quercetin content in bottom phase, and consequently, an increase in the migration of quercetin into the ACN-rich phase.

3.6. Effect of temperature on recovery of quercetin

In Fig. 9C, the effect of temperature has shown on recovery of quercetin in ACN + salt [NaCl/KCl/NaBr/KBr] + water systems. As can be seen, recovery of quercetin decreases with increasing temperature in all systems under investigation and it decrease more significantly for bromide salts. In other words, with decreasing salting-out ability of salt, increasing temperature, the electrostatic interactions between ionic species and water molecules more significantly decreases. Consequently, an increase occurs more significantly in the migration of ACN and quercetin into the salt-rich phase.

3.7. Thermodynamic calculation of quercetin partition

At a given temperature, the change in Gibbs energy (ΔG_t), enthalpy (ΔH_t) and entropy (ΔS_t) of quercetin transfer process can be calculated from the partition data through the following equations [38]:

$$K = \frac{[Q]_{tp}}{[Q]_{bp}} \quad (19)$$

$$\Delta G_t = -RTLnK \quad (20)$$

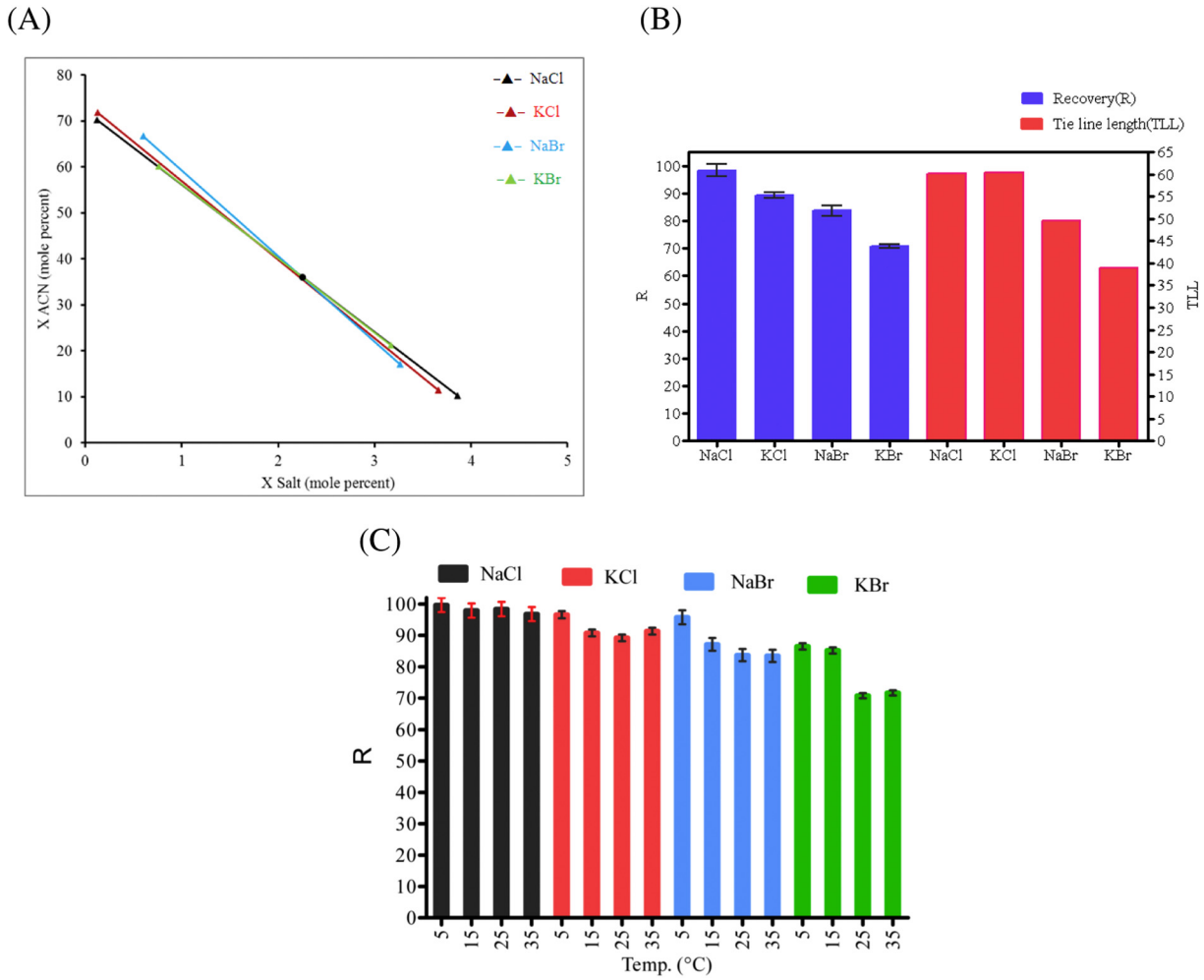

Fig. 9. (A) Comparison of tie lines for the ACN (1) + Salt (2) + Water (3) systems at 25 °C. ●, initial total composition. (B) Comparison of tie lines length and quercetin recovery (R) for same systems at 25 °C. (C) Comparison of quercetin recovery for same systems at different temperatures.

$$\mathrm{LnK} = -\frac{\Delta H_t}{R} \times \frac{1}{T} + \frac{\Delta S_t}{R} \quad (21)$$

where K is partition coefficient of quercetin, R is the gas constant and T is the absolute temperature.

The effect of temperature on the partition behavior of quercetin in ACN (1) + Salt (NaCl, KCl, NaBr, KBr) + water systems was evaluated at different temperatures (5, 15, 25 and 35 °C) and the results were displayed in Fig. 10. and Table 5. From the Eqs. (20) and (21), it is obvious that values of ΔH_t and ΔS_t, can be directly obtained from the slope and intercept of the linear equation between *ln*K and $\frac{1}{T}$, respectively. The calculated ΔG_t values are negative, which reflect the spontaneous and preferential partitioning of quercetin for the ACN-rich phase. The calculated ΔH_t values are negative, which indicated that the transference of quercetin from the salt-rich phase to the ACN-rich top phase is an exothermic process. Fig. 10 compares the partition coefficient of quercetin in $ATPS_s$ studied in this work. The total composition is almost identical for all four systems, but in the same temperature, partition coefficient for chloride salts is more than bromide. In other words, with increasing the salting-out ability of salt, the concentration of quercetin in bottom phase decreases. Based on Fig. 10, it is clear that in the same temperature with increasing the salting-out ability of salt, the calculated ΔG_t values were more negative.

Table 5
The partition coefficient of quercetin (K) with the calculated ΔG_t, ΔH_t and ΔS_t for the ACN (1) + salt (2) + Water (3) systems at different temperatures.

T/K	278.15	288.15	298.15	308.15
System	ACN (1) + NaCl (2) + Water (3)			
K	119.64	49.95	50.78	32.25
$\Delta G(kJ\cdot mol^{-1})$	−11.06	−9.37	−9.74	−8.9
$\Delta H(kJ\cdot mol^{-1})$	−28.1			
$T\Delta S(kJ\cdot mol^{-1})$	−17.04	−18.73	−18.36	−19.2
System	ACN (1) + KCl (2) + Water (3)			
K	57.29	23.95	24.80	12.35
$\Delta G(kJ\cdot mol^{-1})$	−9.36	−7.61	−7.96	−6.44
$\Delta H(kJ\cdot mol^{-1})$	−32.63			
$T\Delta S(kJ\cdot mol^{-1})$	−23.27	−25.02	−24.67	−26.19
System	ACN (1) + NaBr (2) + Water (3)			
K	52.42	15.17	11.64	5.59
$\Delta G(kJ\cdot mol^{-1})$	−9.16	−6.51	−6.08	−4.41
$\Delta H(kJ\cdot mol^{-1})$	−49.95			
$T\Delta S(kJ\cdot mol^{-1})$	−40.79	−43.43	−43.86	−45.54
System	ACN (1) + KBr (2) + Water (3)			
K	17.34	7.95	5.16	3.04
$\Delta G(kJ\cdot mol^{-1})$	−6.60	−4.97	−4.07	−2.85
$\Delta H(kJ\cdot mol^{-1})$	−40.39			
$T\Delta S(kJ\cdot mol^{-1})$	−33.79	−35.42	−36.32	−37.54

4. Conclusion

Phase diagrams of ternary systems (ACN + salt[NaCl/KCl/NaBr/KBr] + water) along with its application have been studied at 25 °C for biomolecule quercetin recovery. The binodal and tie-line data were obtained precisely with simple methods for all selected systems. The salting-out ability of the constituent anions and cations of these salts was in agreement with Hofmeister series. Quercetin was used as a model compound and its distribution behavior was investigated in

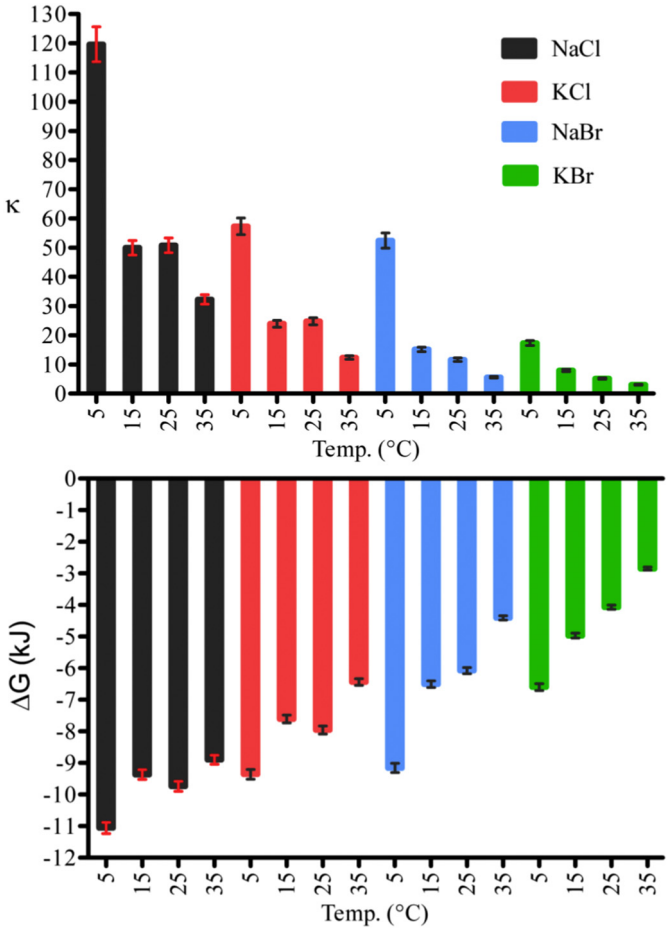

Fig. 10. Effect of temperature on the partition coefficient (K) and ΔG_t of quercetin transfer process in ACN (1) + Salt (2) + Water (3) systems.

aqueous two-phase systems. The CP temperatures data for the investigated systems had shown that the concentration of acetonitrile in equilibrium with a certain concentration of salts significantly increases by increasing temperature. The free energy, enthalpy and entropy of CP were estimated using a simple method. The change in Gibbs energy (ΔG_t), enthalpy (ΔH_t) and entropy (ΔS_t) of quercetin transfer process was calculated from the partition data. The results showed that under the same conditions, with increasing the salting-out ability of salt, IC_{50} values of bottom phases, partition coefficient and recovery of quercetin significantly increased and the calculated ΔG_t values were more negative. It concluded that the driving force of formation of two-phase process may be related to the decrease of enthalpy. The effect of temperature on the recovery of quercetin showed that the efficiency has decreased with increasing temperature in all systems under investigation and the decrease more significantly for bromide salts.

CRediT authorship contribution statement

Safar A. Jafari: Investigation, Data curation, Visualization, Software, Validation, Writing - original draft. **Mohammad H. Entezari:** Supervision, Conceptualization, Methodology, Software, Writing - review & editing.

Declaration of competing interest

The authors declare that they have no known competing financial interests or personal relationships that could have appeared to influence the work reported in this paper.

Acknowledgements

The support of Ferdowsi University of Mashhad (Research and Technology), Iran for this work (3/44919) is appreciated.

Appendix A. Supplementary data

Supplementary data to this article can be found online at https://doi.org/10.1016/j.molliq.2020.113331.

References

[1] A.N. Panche, A.D. Diwan, S.R. Chandra, Flavonoids: an overview, J. Nutr. Sci. 5 (2016) 1–15, https://doi.org/10.1017/jns.2016.41.
[2] M.A. Rostagno, N. Manchón, M.D. Arrigo, E. Guillamón, A. Villares, A. García-lafuente, Fast and simultaneous determination of phenolic compounds and caffeine in teas, mate, instant coffee, soft drink and energetic drink by high-performance liquid chromatography using a fused-core column, Anal. Chim. Acta 685 (2011) 204–211, https://doi.org/10.1016/j.aca.2010.11.031.
[3] M. Russo, C. Spagnuolo, I. Tedesco, S. Bilotto, G.L. Russo, The flavonoid quercetin in disease prevention and therapy: facts and fancies, Biochem. Pharmacol. 83 (2012) 6–15, https://doi.org/10.1016/j.bcp.2011.08.010.
[4] P.C. Hollman, J.H. Vries, S.D. Leeuwen, M.J. Mengelers, M.B. Katan, Absorption of dietary quercetin glycosides and quercetin in healthy ileostomy volunteers, Am. J. Clin. Nutr. 62 (1995) 1276–1282, https://doi.org/10.1093/ajcn/62.6. 1267.
[5] I.F. Mcconvey, D. Woods, M. Lewis, Q. Gan, P. Nancarrow, The importance of acetonitrile in the pharmaceutical industry and opportunities for its recovery from waste, Org. Process. Res. Dev. 16 (2012) 612–624, https://doi.org/10.1021/op2003503.
[6] F. Hofmeister, Zur Lehre von der Wirkung der Salze, Arch. Exp. Pathol. Pharmakol. 24 (1888) 247–260 , Title translation: About the science of the effect of salts https://doi.org/10.1007/BF01918191.
[7] W. Kunz, J. Henle, B.W. Ninham, 'Zur Lehre von der Wirkung der Salze' (about the science of the effect of salts): Franz Hofmeister's historical papers, 9 (2004) 19–37, https://doi.org/10.1016/j.cocis.2004.05.005.
[8] E. Nemati-knade, H. Shekaari, S.A. Jafari, Liquid−liquid equilibrium of some aliphatic alcohols + disodium tartrate + water at 298.15 K, J. Chem. Eng. Data 57 (2012) 2336–2342, https://doi.org/10.1021/je300533r.
[9] T.A. Al-sahhaf, E. Kapetanovic, Salt effects of lithium chloride, sodium bromide, or potassium iodide on liquid - liquid equilibrium in the system water + 1-butanol, J. Chem. Eng. Data 42 (1997) 74–77, https://doi.org/10.1021/je960234r.
[10] Z. Tan, F. Li, X. Xu, Extraction and purification of anthraquinones derivatives from Aloe vera L. using alcohol/salt aqueous two-phase system, Bioprocess Biosyst. Eng. 36 (2013) 1105–1113, https://doi.org/10.1007/s00449-012-0864-4.
[11] Z. Tan, C. Wang, Y. Yi, H. Wang, M. Li, W. Zhou, S. Tan, Extraction and purification of chlorogenic acid from ramie (Boehmeria nivea L. Gaud) leaf using an ethanol/salt aqueous two-phase system, Sep. Purif. Technol. 132 (2014) 396–400, https://doi.org/10.1016/j.seppur.2014.05.048.
[12] I.A.O. Reis, S.B. Santos, F.D.S. Pereira, C.R.S. Sobral, M.G. Freire, L.S. Freitas, C.M.F. Soares, Á.S. Lima, Extraction and recovery of rutin from acerola waste using alcohol-salt-based aqueous two-phase systems, Sep. Sci. Technol. 49 (2014) 656–663, https://doi.org/10.1080/01496395.2013.860461.
[13] Y.X. Guo, J. Han, D.Y. Zhang, L.H. Wang, L.L. Zhou, Aqueous two-phase system coupled with ultrasound for the extraction of lignans from seeds of Schisandra chinensis (turcz.) Baill, Ultrason. Sonochem. 20 (2013) 125–132, https://doi.org/10.1016/j.ultsonch.2012.05.006.
[14] E. Nemati-kande, H. Shekaari, Salting-out effect of sodium, potassium, carbonate, sulfite, tartrate and thiosulfate ions on aqueous mixtures of acetonitrile or 1-methyl-2-pyrrolidone: a liquid-liquid equilibrium study, Fluid Phase Equilib. 360 (2013) 357–366, https://doi.org/10.1016/j.fluid.2013.09.028.
[15] G. De Brito, I. Nascimento, T. Mourão, M.G. Freire, C. Mara, F. Soares, Á. Silva, Novel aqueous two-phase systems composed of acetonitrile and polyol: phase diagrams and extractive performance, Sep. Purif. Technol. 124 (2014) 54–60, https://doi.org/10.1016/j.seppur.2014.01.004.
[16] E. Nemati-knade, H. Shekaari, S.A. Jafari, Thermodynamic study of aqueous two phase systems for some aliphatic alcohols + sodium thiosulfate + water, Fluid Phase Equilib. 321 (2012) 64–72, https://doi.org/10.1016/j.fluid.2012.02.015.
[17] J.C. Merchuk, B.A. Andrews, J.A. Asenjo, Aqueous two-phase systems for protein separation studies on phase inversion, J. Chromatogr. B 711 (1998) 285–293, https://doi.org/10.1016/S0378-4347(97)00594-X.
[18] J. Zhishen, T. Mengcheng, W. Jianming, The determination of flavonoid contents in mulberry and their scavenging effects on superoxide radicals, Food Chem. 64 (1999) 555–559, https://doi.org/10.1016/S0308-8146(98)00102-2.
[19] Y. Athukorala, K. Kim, Y. Jeon, Antiproliferative and antioxidant properties of an enzymatic hydrolysate from brown alga, Ecklonia cava, Food Chem. Toxicol. 44 (2006) 1065–1074, https://doi.org/10.1016/j.fct.2006.01.011.
[20] P.K. Grover, R.L. Ryall, Critical appraisal of salting-out and its implications for chemical and biological sciences, Chem. Rev. 105 (2005) 1–10, https://doi.org/10.1021/cr030454p.
[21] Y. Zhang, P.S. Cremer, Interactions between macromolecules and ions: the Hofmeister series, Curr. Opin. Chem. Biol. 10 (2006) 658–663, https://doi.org/10.1016/j.cbpa.2006.09.020.
[22] S. Shahriari, C.M.S.S. Neves, M.G. Freire, J.A.P. Coutinho, Role of the Hofmeister series in the formation of ionic-liquid-based aqueous biphasic systems, J. Phys. Chem. B 116 (2012) 7252–7258, https://doi.org/10.1021/jp300874u.
[23] S. Moghaddam, E. Thormann, The Hofmeister series: specific ion effects in aqueous polymer solutions, J. Colloid Interface Sci. 555 (2019) 615–635, https://doi.org/10.1016/j.jcis.2019.07.067.
[24] M.T. Zafarani-moattar, S. Hamzehzadeh, Effect of pH on the phase separation in the ternary aqueous system containing the hydrophilic ionic liquid 1-butyl-3-methylimidazolium bromide and the kosmotropic salt potassium citrate at T = 298.15 K, Fluid Phase Equilib. 304 (2011) 110–120, https://doi.org/10.1016/j.fluid.2011.01.023.
[25] Y. Marcus, Thermodynamics of solvation of ions, J. Chem. Soc. Faraday Trans. 87 (1991) 2995–2999, https://doi.org/10.1039/FT9918702995.
[26] A. Dan, S. Ghosh, S.P. Moulik, The solution behavior of poly (vinylpyrrolidone): its clouding in salt solution, solvation by water and isopropanol, and interaction with sodium dodecyl sulfate, J. Phys. Chem. B 112 (2008) 3617–3624, https://doi.org/10.1021/jp077733r.
[27] J. Setschenow, Über die konstitution der salzlösungen auf grund ihres varhaltens zu kohlensa üre, Z. Phys. Chem. 4 (1889) 117–125, https://doi.org/10.1515/zpch-1889-0409.
[28] Y. Tang, Y. Li, Salting effect in partially miscible systems of n-butanol-water and butanone-water, Fluid Phase Equilib. 105 (1995) 241–258, https://doi.org/10.1016/0378-3812(94)02616-9.
[29] M.J. Hey, D.P. Jackson, H. Yan, The salting-out effect and phase separation in aqueous solutions of electrolytes and poly(ethylene glycol), Polymer 46 (2005) 2567–2572, https://doi.org/10.1016/j.polymer.2005.02.019.
[30] H. Shekaari, R. Sadeghi, S.A. Jafari, Liquid - liquid equilibria for aliphatic alcohols + dipotassium oxalate + water, J. Chem. Eng. Data 55 (2010) 4586–4591, https://doi.org/10.1021/je9008188.
[31] A. salabat, M. Hashemi, Temperature effect on the liquid-liquid equilibria for some aliphatic alcohols + water + K2CO3 systems, J. Chem. Eng. Data 51 (2006) 1194–1197, https://doi.org/10.1021/je050515b.
[32] S.M. Arzideh, K. Movagharnejad, M. Pirdashti, Influence of the temperature, type of salt, and alcohol on phase diagrams of 2-propanol + inorganic salt aqueous two-phase systems: experimental determination and correlation, J. Chem. Eng. Data 63 (2018) 2813–2824, https://doi.org/10.1021/acs.jced8b00160.
[33] Y. Li, Y. Zhao, R. Huang, Q. Cui, X. Lu, H. Guo, A thermodynamic study on the phase behaviour of ethanol and 2-propanol in aqueous ammonium sulphate/sodium sulphate solution, J. Mol. Liq. 211 (2015) 924–933, https://doi.org/10.1016/j.molliq.2015.08.021.
[34] M.T. Zafarani-Moattar, H. Shekaari, P. Jafari, Design of novel biocompatible and green aqueous two-phase systems containing Cholinium L-alaninate ionic liquid and polyethylene glycol di-methyl ether 250 or polypropylene glycol 400 for separation of bovine serum albumin (BSA), J. Mol. Liq. 254 (2018) 322–332, https://doi.org/10.1016/j.molliq.2018.01.094.
[35] E. Nemati-kande, H. Shekaari, S.A. Jafari, Liquid – liquid equilibrium of 1-propanol, 2-propanol, 2-methyl-2-propanol or 2-butanol + sodium sulfite + water aqueous

two phase systems, Fluid Phase Equilib. 329 (2012) 42–54, https://doi.org/10.1016/j.fluid.2012.05.012.
[36] M. Bancirova, Changes of the Quercetin Absorption Spectra in Dependence on Solvent, 1, 2015 31–34.
[37] R. Sokolováa, I. Deganob, S.R. sováa, J.B. ckováa, M. Hromadováa, M. Gála, J. Fiedlera, M.V. sekc, The oxidation mechanism of the antioxidant quercetin in nonaqueous media, Electrochim. Acta 56 (2011) 7421–7427, https://doi.org/10.1016/j.electacta.2011.04.121.
[38] L. Yan, Y. Sun, X. Wang, H. Fu, Y. Mu, Z. Xiu, Partition behavior of monocarboxylic acids in salting-out extraction systems of monohydric alcohols and dipotassium phosphate, Sep. Purif. Technol. 199 (2018) 351–358, https://doi.org/10.1016/j.seppur.2018.02.006.